ATLAS Internal Note
MUON-NO-177

September 1 1997

High Rate Performance of MDTs

G.Scherberger, V.Paschhoff, V. Waldmann,
U. Landgraf, G. Herten, W. Mohr
University of Freiburg*, Germany

September 97

ABSTRACT

This note describes calculations and measurements of space charge effects in the MDTs. Two main items are studied: the reduction of the gas gain and disturbances of the drift field, both resulting from slowly drifting positive ions.
Whereas the modification of the electric field is independent of the gas, the magnitude of changes to the r-t relation is very different for linear and nonlinear gases. The gas has to be chosen carefully to avoid significant effects at ATLAS operating conditions.

*Address: Fakultät für Physik, Hermann-Herder-Str. 3, 79104 Freiburg i. Br., Germany
e-mail: Gunter.Scherberger@cern.ch

1 Introduction

The electric field inside a tube with radius b and wire radius a held at potential V can easily be calculated:

$$E(r) = \frac{V}{\ln \frac{b}{a}} \cdot \frac{1}{r} \tag{1}$$

This formula is only correct if one can neglect the electric charges that are produced in the avalanche process. At high particle rates or high gas gain, one expects a decreased electric field near the signal wire because of positive ions screening it. This will lead to a lower gas gain which means lower pulse height. Since the voltage between wire and tube is fixed, the electric field at large radius is increased if the field near the wire is decreased due to space charge effects. Figure 1 compares the E-field of a MDT with and without the addition of space charges coming from a muon rate of 3000 Hz/cm^2. The tube is operated at a gain of $2 \cdot 10^4$ at a pressure of 3 bar with the gas Ar-CH_4-N_2 91-5-4 %. One can clearly see that the field for drifting electrons is changed. As the drift velocity depends on the electric field, the time to drift a certain distance will be different: the r-t relation changes with rate. The magnitude of this effect depends on the variation of the drift velocity with E, which is strongly dependent on the gas.

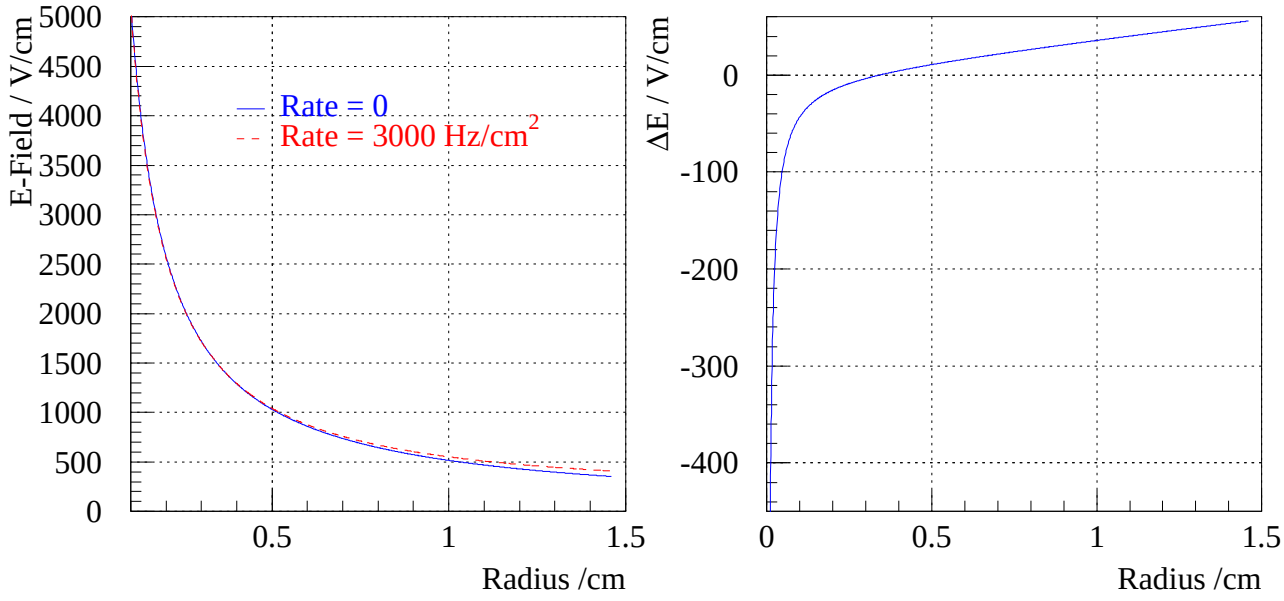

Figure 1: Comparison of the electric field inside a tube with and without space charges. Left: E-Field plotted for $r \geq 1$ mm, right: difference of the electric fields. The field near the wire which is relevant for the gas amplification is decreased whereas the field for the drifting electrons is increased for $r > 4$ mm.

2 Calculation of Field Disturbances

The density of the space charges coming from positive ions can be calculated making the following simplifications:

- the irradiation is homogeneous within one tube.
- fluctuations in rate are ignored.

For low irradiation rates, the second assumption will no longer be justified: The space charge density will depend on the time and the position of the last muon that passed the tube. If e.g. this time is longer than the maximum ion drift time, all space charges are gone. However, the mean value of the charge density will be correct.

The drift velocity w of the positive ions is proportional to the reduced electric field

$$w = \mu \cdot \frac{E}{p} \quad , \tag{2}$$

the constant μ is called the mobility of the gas. The electric field inside a tube is given by (1). The maximum ion drift time t_+ (which is the drift time for almost all ions because nearly all of them are produced at the wire) is obtained by integrating (2),

$$t_+ = \frac{b^2 p \ln \frac{b}{a}}{2\mu V} \quad . \tag{3}$$

Note that for the calculation of the above formula the electric field (1) of the undisturbed tube is used. For high rates, the electric field will change and the maximum ion drift time has to be corrected, as will be shown below.
As shown in [1]*, the charge density is independent of the radius in case of a cylindric tube geometry and $w \propto 1/r$.

$$\rho(r) = \rho = n_p \cdot g \cdot t_+ \frac{1}{\pi b^2} \cdot \frac{R}{L} \tag{4}$$

with n_p = the number of primary ion pairs (the number of pairs before gas amplification), g is the gas amplification factor and R/L is the particle rate per wire length. The potential $\Phi(r)$ can now be calculated with Poisson's equation

$$\nabla^2 \Phi = -\frac{\rho e}{\varepsilon_0} \qquad \text{(mksa units)} \tag{5}$$

and the boundary conditions $\Phi(a) = V$ and $\Phi(b) = 0$.

$$\Phi(r) = \frac{V \ln \frac{b}{r}}{\ln \frac{b}{a}} + \frac{\rho e}{4\varepsilon_0} \left[\left(b^2 - r^2 \right) - \frac{(b^2 - a^2) \ln \frac{b}{r}}{\ln \frac{b}{a}} \right] \tag{6}$$

*in that publication, the results are wrong by a factor of π

Thus

$$E(r) = -\nabla\Phi(r) = \frac{V}{\ln\frac{b}{a}} \cdot \frac{1}{r} + \frac{\rho e}{4\varepsilon_0}\left[2r - \frac{b^2 - a^2}{\ln\frac{b}{a}} \cdot \frac{1}{r}\right] \quad . \tag{7}$$

This is the formula that has to be taken instead of (1).
For calculations of the gas gain, only the field near the wire has to be known. In this case, the above formula can be simplified to

$$E(r) = \frac{V - \delta V}{\ln\frac{b}{a}} \cdot \frac{1}{r} \qquad (a \le r \ll b) \tag{8}$$

where

$$\delta V \quad = \quad \frac{\rho e b^2}{4\varepsilon_0} \quad = \quad n_p \cdot g \cdot t_+ \cdot \frac{e}{4\pi\varepsilon_0} \cdot \frac{R}{L} \quad . \tag{9}$$

The electric field in the avalanche region behaves as if the effective voltage at the wire was $V - \delta V$.

Taking now a model for the gas amplification where the gas gain is a function of the applied voltage, one should be able to describe the dependence of the gas gain reduction as function of rate. We will use the Diethorn formula [2]

$$g = \exp\left[\frac{V \ln 2}{\Delta V \ln\frac{b}{a}} \cdot \ln\frac{V}{K\frac{p}{p_0} a \ln\frac{b}{a}}\right] \quad . \tag{10}$$

Diethorn uses two parameters ΔV and K which are characteristic for every gas mixture. ΔV is the potential difference an electron passes between two successive ionisations and K is the critical value of E/p where ionisation starts. p/p_0 is the fraction of the actual pressure p to the reference pressure p_0 where K was determined.
For calculating the actual gas gain at rate R/L, one now has to replace V by $V - \delta V$ in (10) where δV is given by (9). Note that δV depends on the gain and vice versa. The two equations can be solved in an iterative way to get a self consistent gain for every rate.

One more correction has to be made for high rates: the maximum ion drift time t_+ in (9) depends on the rate which was ignored in (3). For a better approximation of t_+, one can insert into (2) the electric field (7) which leads to the formula

$$t_+ = \frac{p\varepsilon_0}{\mu\rho e} \cdot \ln\left[1 + \frac{\rho e b^2 \ln\frac{b}{a}}{2\varepsilon_0 (V - \delta V)}\right] . \tag{11}$$

In the limit of rate $\to 0$, this is identical to (3).
To apply this correction, one needs to have a good starting value of ρ (4) and δV (9) and iterate the calculations several times. Figure (2) shows the decrease of the maximum ion drift time with increasing rate for the gas Ar-CH_4-N_2 91-5-4 % operated at a gas gain of $2 \cdot 10^4$. The input values $\Delta V = 62.1$ V and $K = 13$ kV/cm where fitted to gas gain measurements from [3].

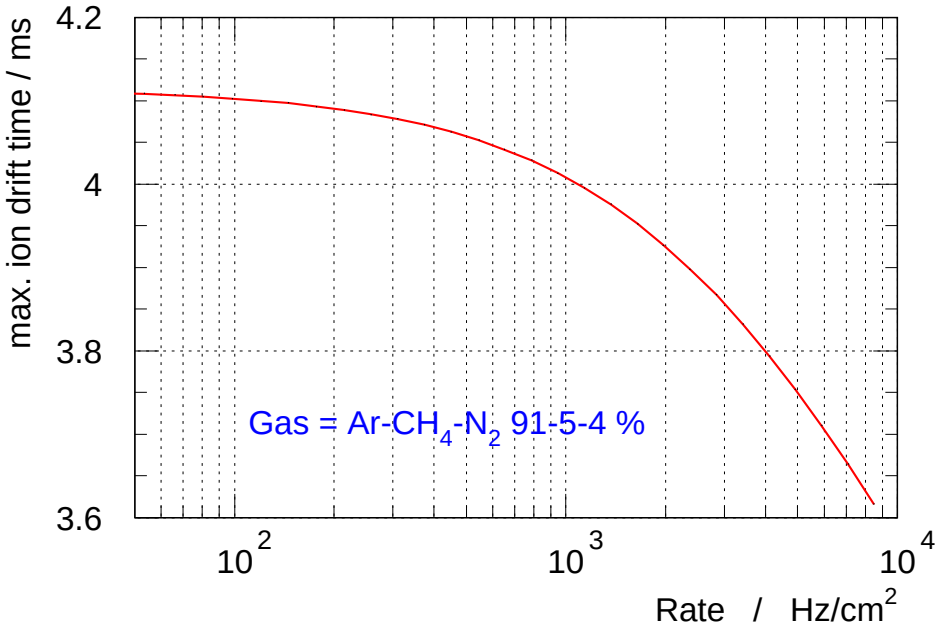

Figure 2: Change of the maximum ion drift time with rate. Calculation with (11).

3 Experimental Setup

To measure effects of high rates, a specially designed chamber was built for operation in the M2 muon beam at CERN. The task of this setup was to see only effects coming from space charges and to avoid measuring electronic effects such as saturation of preamplifiers etc. A picture of the apparatus is shown in fig. 3. The chamber consists of 24 drift tubes: two bundles of eight tubes with 3 cm diameter, two tubes with 2 cm and two tubes with 4 cm diameter. The tubes are glued together precisely, and the two bundles are staggered to improve track fitting. For measuring the second coordinate, four tubes are placed perpendicular to the others. All tubes are 30 cm long, but the active length is only 4 cm in the middle part for the vertical tubes (=precision coordinate) and 10 cm active length for the second coordinate tubes (fig. 5). In order to passivate the rest of the tube, the wires have been coated galvanically with silver to increase the wire diameter from 50 μm to 150 μm to avoid gas amplification. The trigger is made of a coincidence of four scintillation counters which cover an area of 1 cm (along the wires) $\times$ 6 cm (= two tubes in height) and are placed in the middle of the active part of the tubes.

The whole setup can be moved horizontally by a stepper motor within a range of 1 m towards the centre of the M2 muon beam. By moving the apparatus with respect to the muon beam one can adjust the trigger rate from 10 Hz/cm^2 up to more than 10 kHz/cm^2.

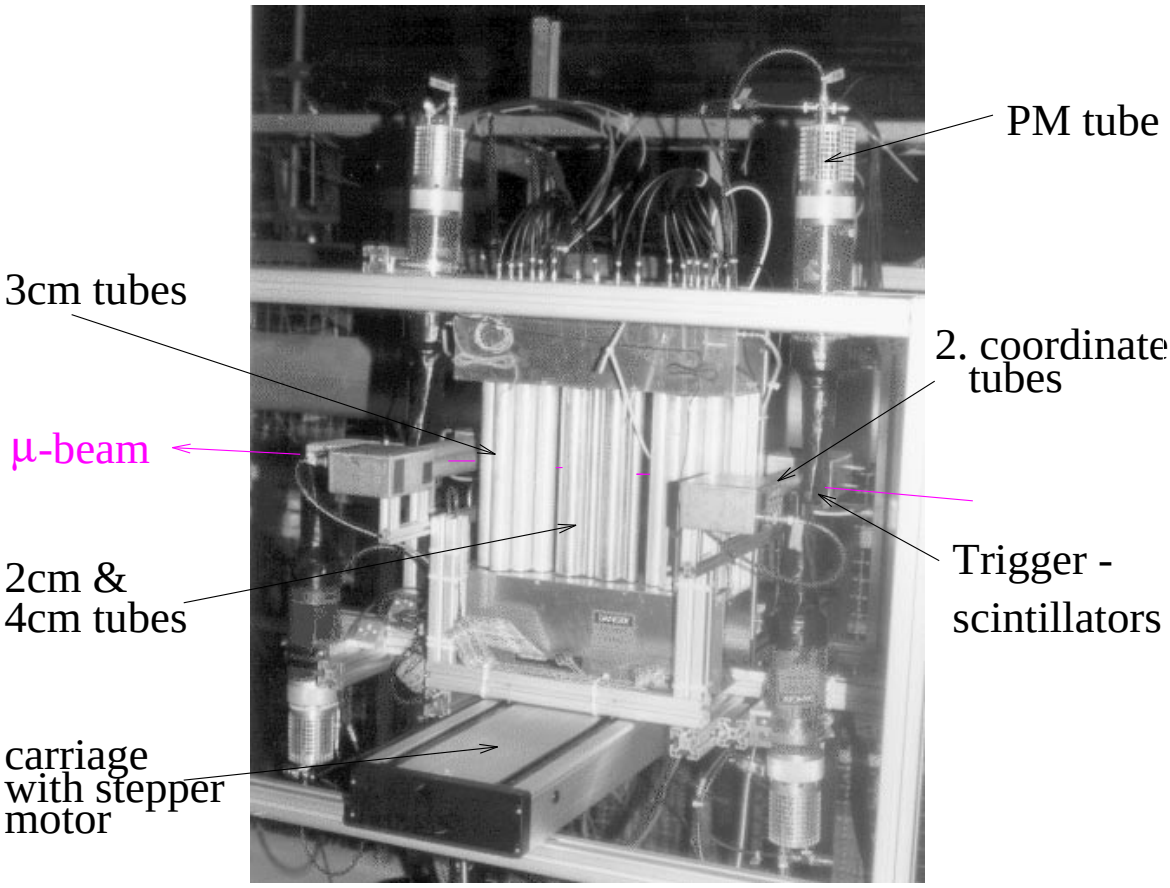

Figure 3: Photo of the apparatus in the M2 muon beam at CERN. One can see two bundles of 3 cm diameter tubes, 2 tubes with 2 cm and 2 tubes with 4 cm diameter. In order to measure the second coordinate, there are 2 tubes perpendicular to the others at each side of the chamber. The trigger is very small, covering only an area of 1 × 6 cm^2 in the sensitive zone of the tubes.

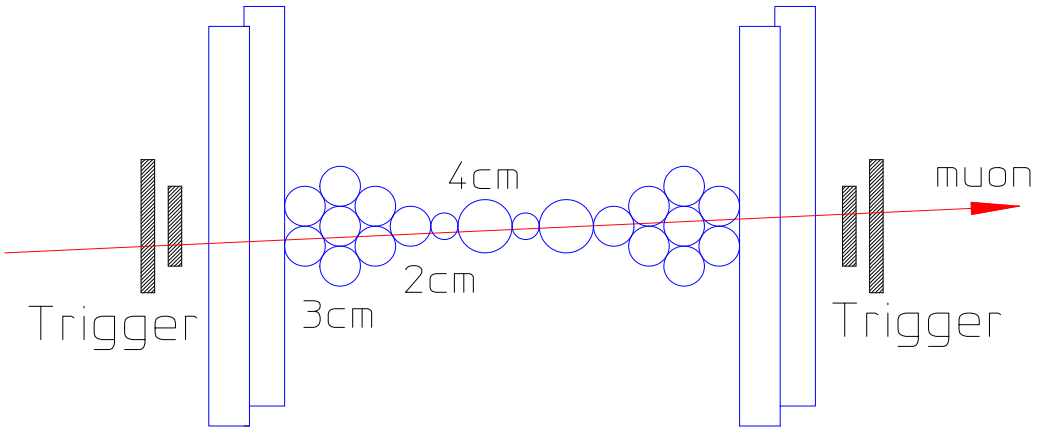

Figure 4: Schematic drawing of the chamber, view from top

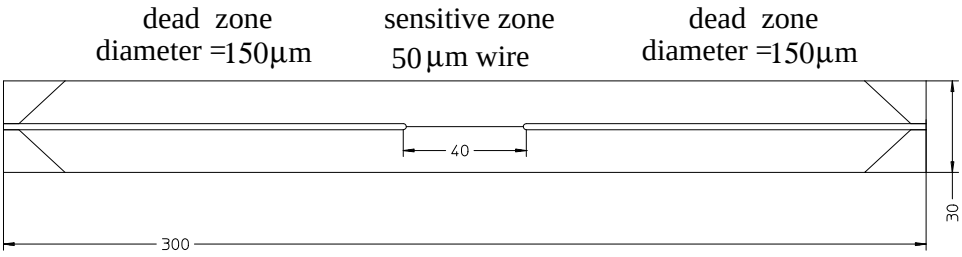

Figure 5: Setup of a single tube. The wire is coated to avoid gas amplification except for some length in the middle part

4 Data Readout and Analysis

Whereas for ATLAS the tubes will be read out with TDCs, here the whole analog pulse information was read out with 250 MHz Flash-ADCs [4]. This is necessary for measuring pulse height reductions and to be independent of a fixed chosen discriminator threshold.
An important difference to most of the other test measurements done with MDTs is that the data acquisition was able to record at least 8 successive tracks without loosing one. This is necessary for the calculation of the particle rate in each tube and for observing effects coming from statistical fluctuations of rate where the "history" of the tube has to be known.
In order to achieve this deadtimeless readout, a trigger logic has been set up that does not need any VME or CAMAC cycle between the first and 8th event trigger. The memory depth of the FADC is 2048 corresponding to 8192 ns in time which is large enough to store 8 waveforms of MDT pulses (fig. 7). The digitization of the Flash-ADCs is started (and stopped after

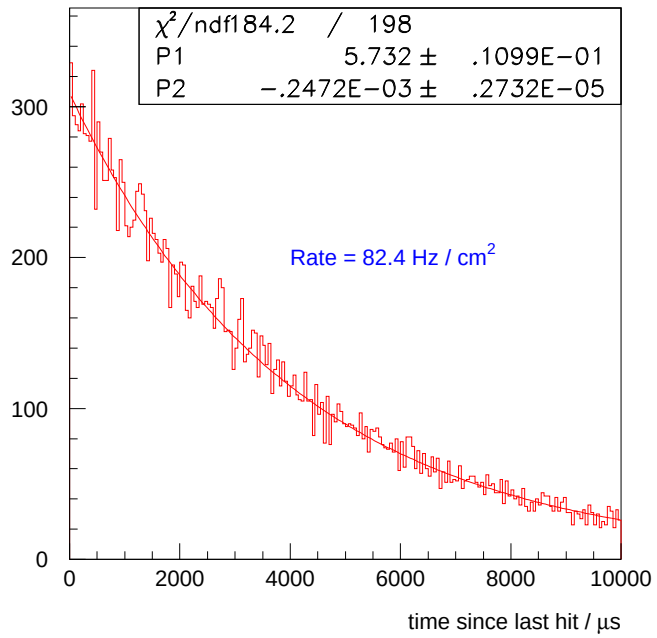

Figure 6: Time differences between two hits in a tube. Fitted to the data is an exponential function $f(t) = \exp(p_1 + p_2 t)$.

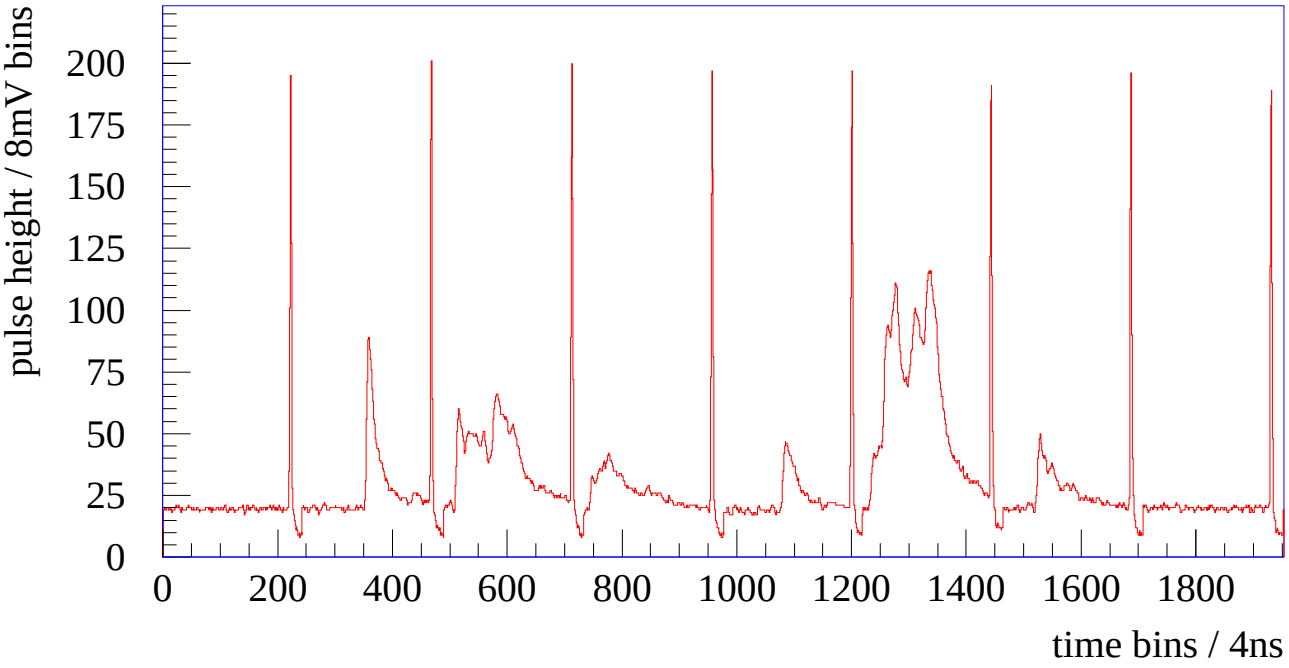

Figure 7: Memory content of one FADC channel. One can see 8 waveforms (some are empty) of pulses coming from the same tube but from 8 successive events. At the end of each section there is a narrow but high reference pulse needed for separating the different pulses and as an exact time marker for drift time measurements

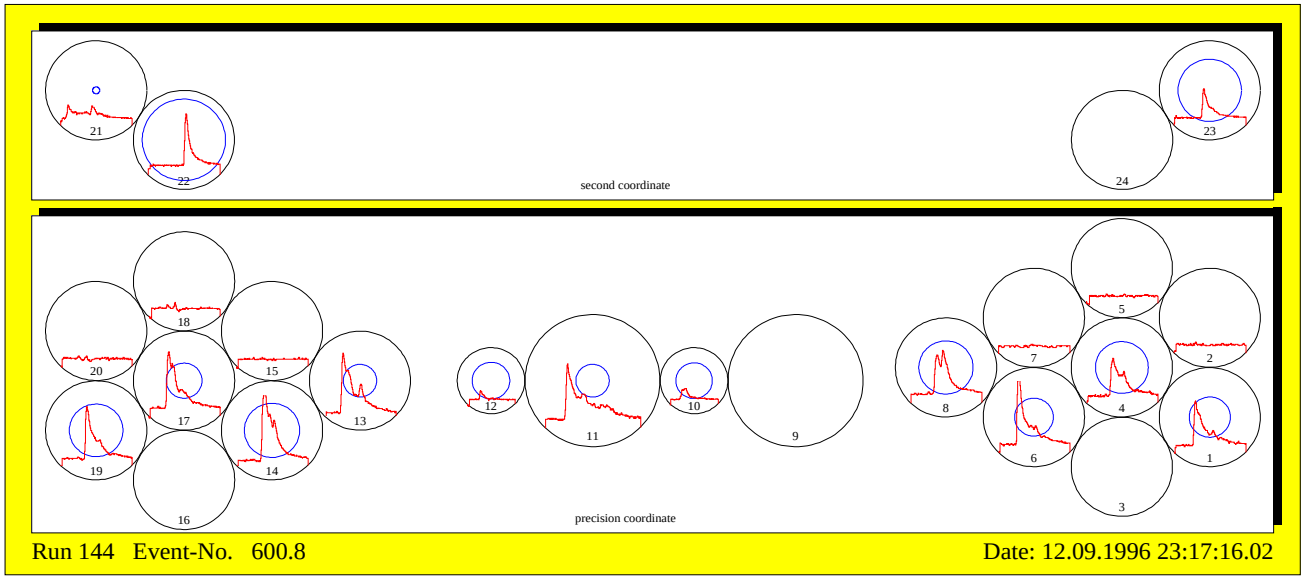

Figure 8: Event display of a muon traversing the chamber. The upper part shows the second coordinate tubes. The circles inside a tube indicate the reconstructed drift distance if a pulse was found. The empty tubes have not been read out.

$1\,\mu$s) with a NIM signal for each new muon trigger.

The time differences between successive triggers were measured with a setup of slow TDCs (5 MHz clock) covering a time range of $\approx$ 20 ms. With this information it is possible to compute for every tube the time differences to the last hit and the rate. The distribution of these times is exponential (fig. 6) and one can fit the function $\exp(p_1 + p_2 \cdot t)$. The mean value is $\langle t \rangle = \frac{-1}{p_2}$ (as can be shown easily) , in agreement with the number of triggers per second counted with a scaler. With this measurements we know both, the time since the last muon went through a tube and (from the second coordinate measurements) the spatial distance along the wire to the last particle.

The amount of data that had to be read out was rather big. A typical size is 40k for every readout cycle (8 events). The data were processed by a VME processor running under OS 9 and stored on an exabyte tape. To maximize the readout speed, all time critical routines have been written in assembler code. The maximum readout rate that could be achieved (if the particle rate was high enough) was $\approx$ 800 events within one spill of the SPS (2.4 s beam followed by a pause of 12 s) and was limited by the speed of the tape drive. The time needed to get a high statistics run (800k triggers) at highest rates was 4 hours.

The measurement of drift times with this kind of FADC is problematic. The time difference between incoming start signal and start of the digitization can be up to 12 ns. In order to get a precise time marker, the trigger signal that starts the readout was delayed by 800 ns and fed into the test input of the preamplifiers FBPANIK-04 [5]. Thus, every drift chamber pulse (even if it was empty) was followed by a reference pulse coming always with the same delay to the muon trigger (fig. 7). So the time difference between the pulse and the reference pulse is the drift time (plus a constant offset t_0).
The time bins of the FADCs have a width of 4 ns. To get a better time resolution of the pulse, the DOS (difference of samples) method [6],[7] was used which was developed for the analysis of the FADC data from the OPAL experiment. This method is numerically rather simple but very efficient in both finding pulses and calculating the exact drift time. First, the pulse shape is differentiated by subtracting the pulse heights of successive bins. Then pulses can be found if the differentiated pulse reaches a certain threshold. Finally the drift time is calculated as the weighted mean of the differentiated pulse around the position of the maximum of the differentiated pulse.
An event display of a muon passing the chamber is shown in fig. 8.

5 Pulse Height Reductions

In order to measure the correct gain drop that is only due to particle rate one has to take care of several effects that influence the measured pulse height. First of all, only data from the same tube are compared.

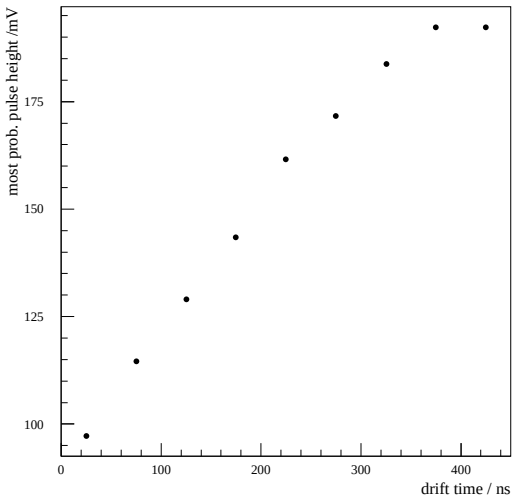

Figure 9: The pulse height depends on the drift distance. This is due to the different pulse shapes (at the same total charge) of pulses coming from short and long drift distances. Measurement done with the gas Ar-CH_4-N_2 91-5-4 % at 3 bar and gas gain of $2 \cdot 10^4$.

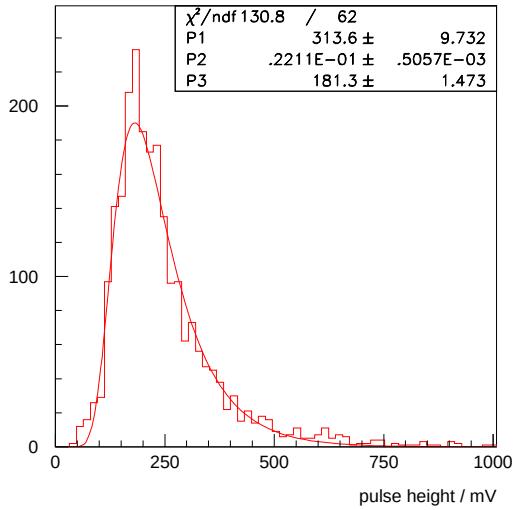

Figure 10: Histogram of the maximum pulse heights of measured MDT pulses. A Landau function is fitted to this distribution to determine the most probable pulseheight (parameter P3 of the fit).

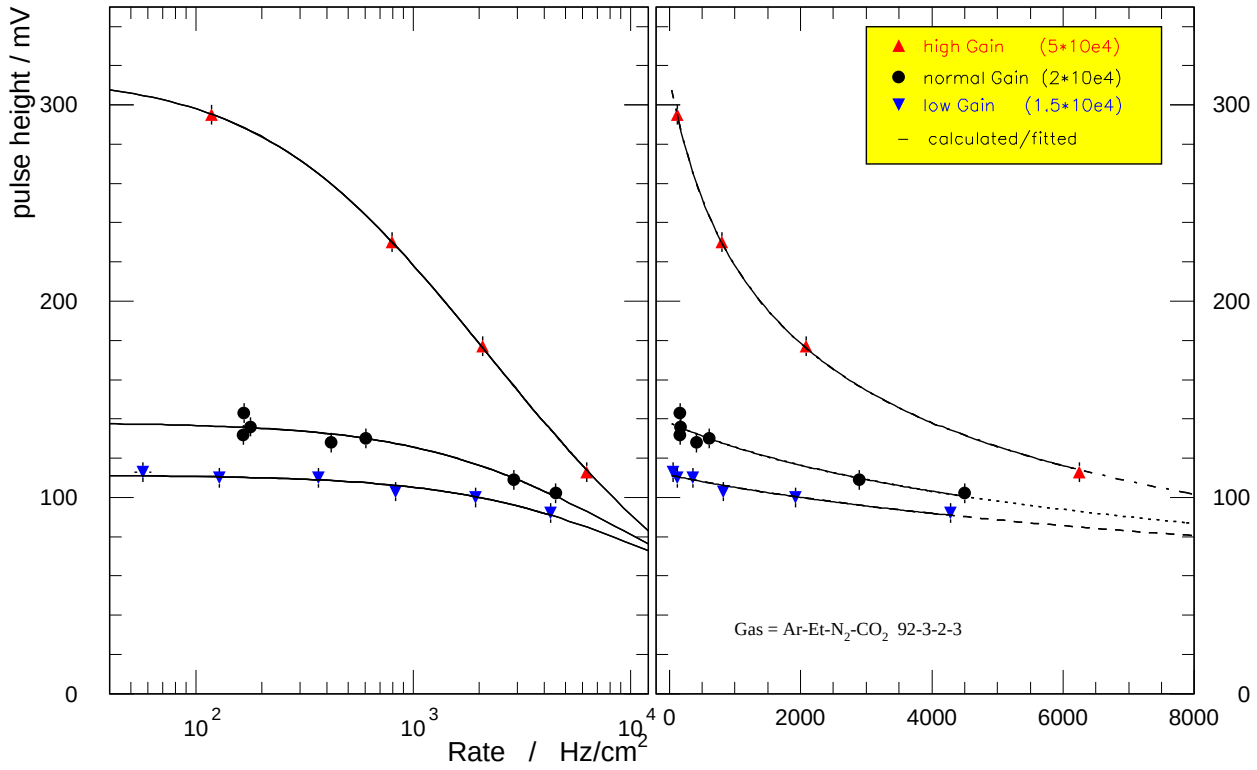

Figure 11: Degradation of the Pulse height with rate. Left: rate is plotted logarithmically, right: linearly. The extrapolation shows that the three curves join at rates ≥ 15 kHz/cm^2.

One important quantity is the temperature of the gas. The pulse height increases with temperature if the pressure is kept constant. The order of magnitude of this effect is some percent per Kelvin. So either one has to take all the data at the same temperature (which is impossible in an non air-conditioned hall), ore one has to correct the data for the temperature changes which was done here.
However, the most important point is to make a cut on the drift time. As can be seen in fig. 9, the measured pulse height increases with drift time (with distance from the wire). Pulses with a short drift time have a lower maximum and a longer tail compared to those with long drift time - at same total charge. A cut on the drift time was applied to ensure that only pulses coming from long drift distances were used, also the last 1.5 millimeters of drift distance were cut away to avoid effects of the wall.

After these cuts, the maximum of each pulse was determined and histogramed. Because muons are minimum ionising particles, the distribution of the pulse heights follows a Landau function [8] which was fitted to the data. This is shown in fig. 10. To describe the distribution of the pulse heights, the most probable pulse height (which is one parameter of the fit) was used and not the mean value of the data sample (which is bigger). In the following pulse height means the most probable pulse height of the Landau fit.

Fig. 11 shows the behaviour of the pulse height with increasing rate for 3 different settings of the high voltage, corresponding to gas gains of $1.5 \cdot 10^4$, $2 \cdot 10^4$ and $5 \cdot 10^4$ at zero rate.
The solid lines show a calculation of the pulse height. The Diethorn formula (10) was used to calculate the gain drop. The parameters ΔV and K have been fitted to low rate data where the pulse height was measured for different high voltages.
For the calculation of the electric field (7) and the actual gain, several iterations of the calculation of δV (9), the gas gain (10) and the maximum ion drift time (11) are necessary to obtain a correct (self-consistent) value for the charge density ρ (4). To compare measured pulse height and calculated gain, one parameter was fitted to the data: the ion mobility μ. It was found that this value was identical within the errors for all the measured gases and it is also consistent with the mobility of Ar^+ ions in Ar found in [9],[10]: $\mu = 1.5 \frac{cm^2 bar}{Vs}$.

One can see that for initial high gas gain, the pulse height drops rather fast with increasing rate, going down to 30% of its initial value at 8 kHz/cm^2. For standard ATLAS conditions with a gas gain of $2{\cdot}10^4$ and rates $\leq$ 100 Hz/cm^2 the behaviour is rather uncritical, the reduction is some 10%.
However, at very high rates, the pulse height is more and more independent of the high voltage, the electric field is reduced to the same value due to space charge effects. The order of magnitude of the gain drop with rate is roughly the same for different gases. The gain drop is worse for gases with low working point (low high voltage for the same gas gain) because in that case, the ion drift time is longer and so the space charge density is bigger.

6 Changes in the Electron Drift Time

The electric field for drifting electrons is changed with rate according to (7). Whereas the field is more or less the same for different gases at the same rate (at least if they have to be operated at the same high voltage), the changes to the electron drift times are different. The drift time is given by

$$t(r) = \int_a^r \frac{dr'}{v(E(r'))} \quad . \tag{12}$$

As the drift velocity depends on the electric field, it will change if the field is disturbed. The change in drift time depends on the slope of the drift velocity $v(E)$ with the electric field. If the drift velocity is constant, changes in the field cause no changes in the drift time. A gas becomes faster with rate if the slope is positive and slower if it is negative.
One can see here that in order to keep the drift time changes small one has to look for gases with constant drift velocity, so called linear gases (linear because in this case, the r-t relation is a straight line). Fig. 13 shows the drift velocities and fig. 14 the corresponding r-t relations for three gases that have been studied experimentally: the rather linear DATCHA gas (Ar-CH_4-N_2 91-5-4 %), the very linear gas Ar-Ethane-N_2-CO_2 94-3-2-1 % and the semi-linear Ar-Ethane-N_2-CO_2 92-3-2-3 %. For comparison, the non-linear gases Ar-CO_2 80-20 % and Ar-CO_2 90-10 % are added.

To study the effects of the modified electric field, we look at the change of the maximum electron drift times at different irradiation rates.
The calculation of the maximum drift time can be done with (12) with r = radius of the tube. To do this, one needs to know the drift velocity $v(r)$ of the gas mixture. As no measurements

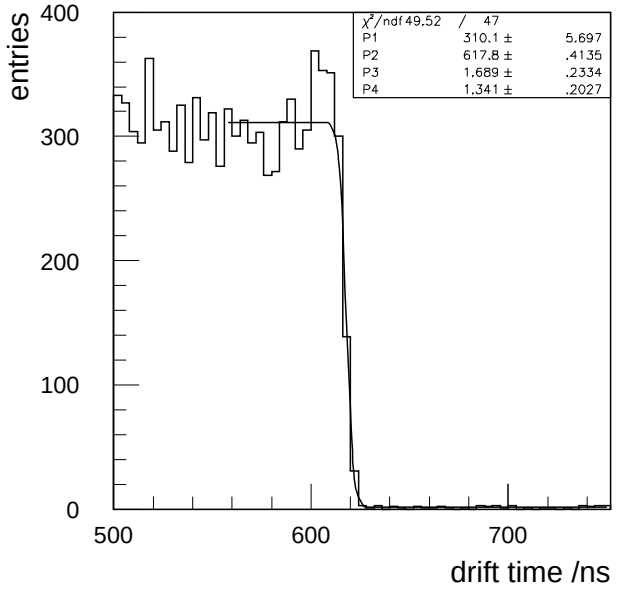

Figure 12: Fit of the maximum electron drift time. A Fermi function is fitted to the end of the drift time distribution.

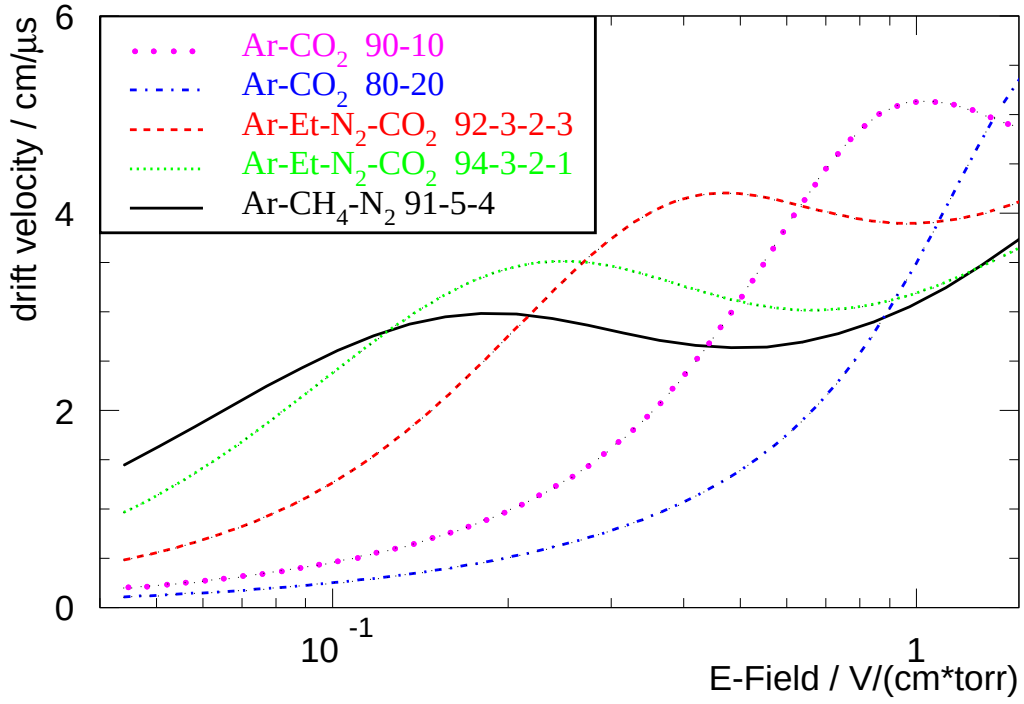

Figure 13: Comparison of the drift velocity for different gases. The typical range of the E-Field inside a drift tube is from 0.15 V/(cm torr) (at the wall of the tube) up to 1.1 V/(cm torr) (2 mm from the wire)

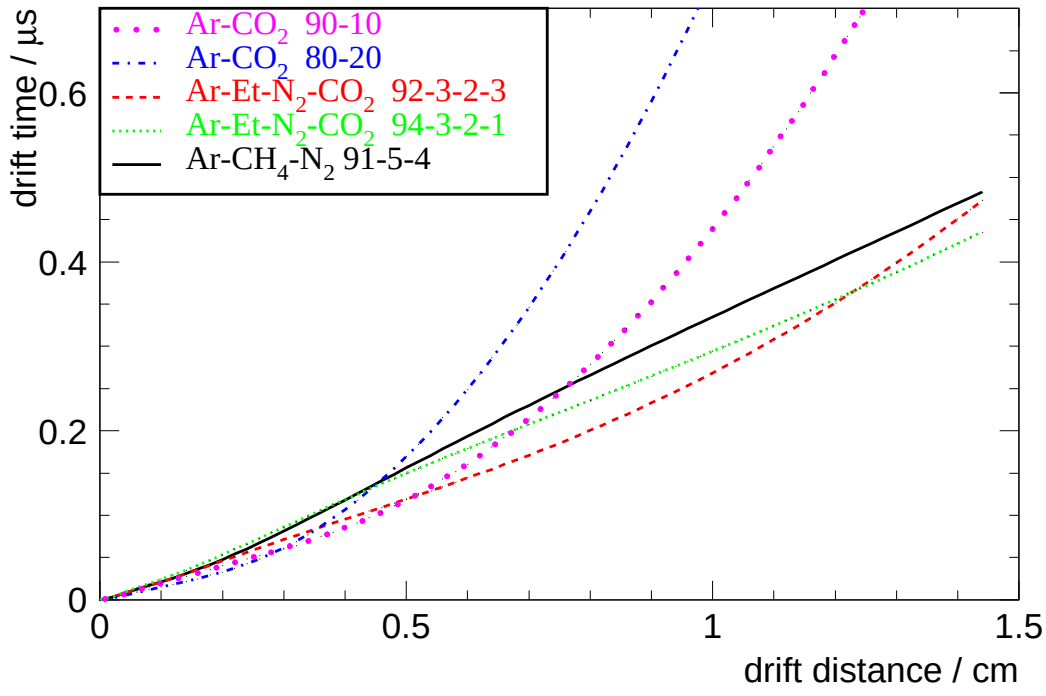

Figure 14: R-T relations for the gases shown in fig. 13. Gases with linear r-t relation have a rather constant drift velocity in the relevant region of E/p compared to the other gases.

were available, the MAGBOLTZ [16] program was used to calculate the drift velocity as function of the reduced electric field $v(\frac{E}{p})$. Eq. (7) was taken to calculate the correct electric field $E(r)$ and then the new r-t relation was integrated with (12).
For using the equation (7) the same numbers for the charge density (and the ion mobility) were used as for the calculation of the gain drop in the previous section. The calculated maximum drift time is shown as lines in fig. 15, together with the measured points.

The maximum electron drift time of the measured data can be determined from the end of the distribution of the drift times. Because of diffusion and effects at the wall of the tube, the end is smeared. To get a precise and reproducible number, a Fermi function is fitted to the distribution ([11]). Parameters of the fit are the high and low level, the speed of decreasing and the time of half height. The last one is taken as the maximum drift time. The physical maximum drift time may be different from this value by a constant offset, but this is unimportant since we are only interested in changes of the maximum drift time.
The results are plotted in fig. 15. Three gases are shown there: the linear DATCHA gas (Ar-Methane-N_2 91-5-4 %) and the non-linear gas with the same maximum drift time Ar-Ethane-N_2-CO_2 92-3-2-3 % and the very linear gas Ar-Ethane-N_2-CO_2 94-3-2-1 %. For the DATCHA gas, the max. drift time is stable up to very high rates with a tendency to increase with rate. The non-linear one shows already differences of several nanoseconds at ATLAS conditions (100 Hz/cm^2). Note that these measurements have been done with muons whereas in ATLAS the radiation background [12] will be dominated by photons which produce on average a factor of 2 more primary ion pairs. If one is interested in the behaviour at a photon rate of 100 Hz/cm^2, one has to look at a muon rate of 200 Hz/cm^2 to get the correct value.
Surprisingly, both measurement and calculation show that the gas with the most linear r-t relation is not the best one. The reason for this is the fact that the operation point of Ar-Ethane-N_2-CO_2 94-3-2-1 is much lower compared to the others (2575 V instead of 3300 V for DATCHA). This lower voltage has two effects:

- the amount of space charge is proportional to the inverse of the voltage.
  $\rho \propto t_+ \propto \frac{1}{V}$ because of (4) and (3).
- the relative change of the electric field is proportional to the inverse square of the voltage
  $\frac{\Delta E}{E} \propto \frac{1}{V^2}$ because of (7).

Both items show that the optimum gas should have an high operational voltage. The reason for the relative low working point of this gas is the use of Ethane as quencher. By replacing it with Methane, this will change (see below).
Fig. 16 shows the same calculation as fig. 15 for low rates in a linear scale. Additionally, calculations for the gases Ar-CO_2 80-20 % and 90-10 % are shown for comparison with non-linear gases. The required input parameters ion mobility and gas gain versus high voltage curve are taken from [13] and [14] respectively.

The relevant number concerning resolution loss of the MDTs is not the change in the maximum drift time, but the mean position error. This number is calculated as the rms of the differences

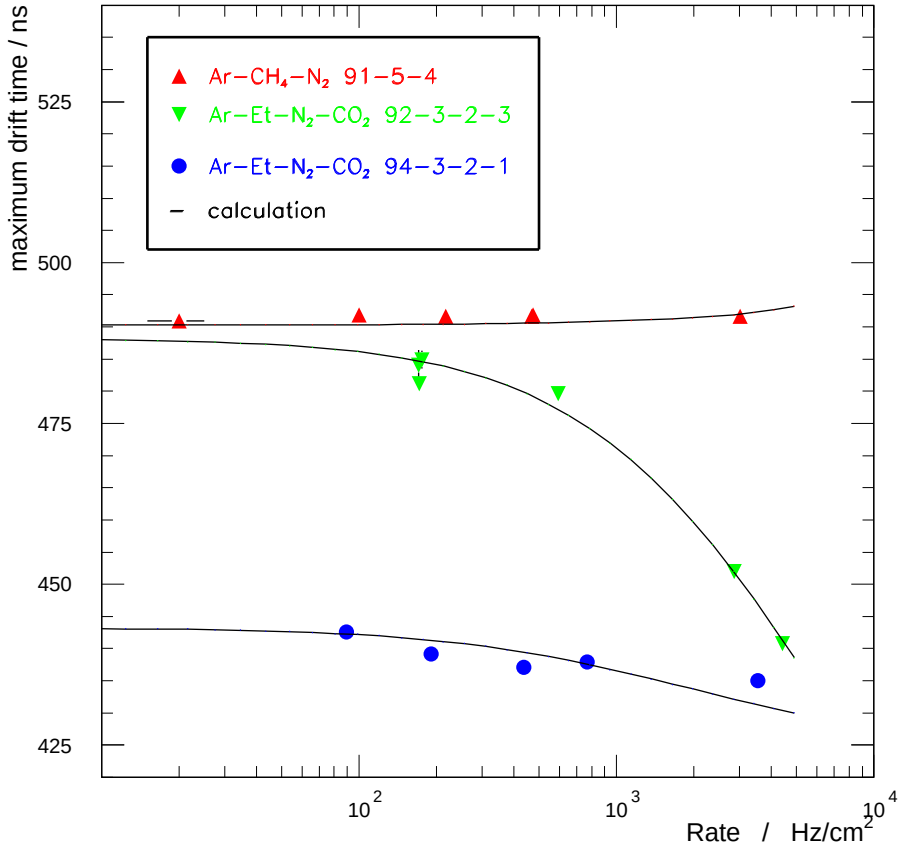

Figure 15: Comparison of measured change in the maximum electron drift time and calculation

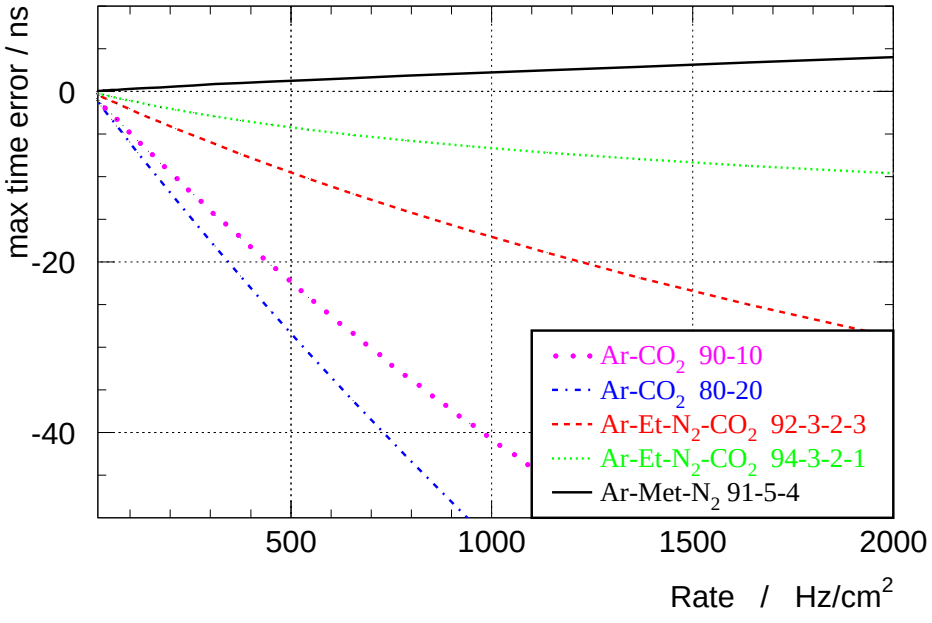

Figure 16: Change of the maximum drift time with rate. The calculation is the same as in the previous plot. For comparison, the calculated behaviour of the very non-linear gases Ar-CO_2 80-20 % and Ar-CO_2 90-10 % are added.

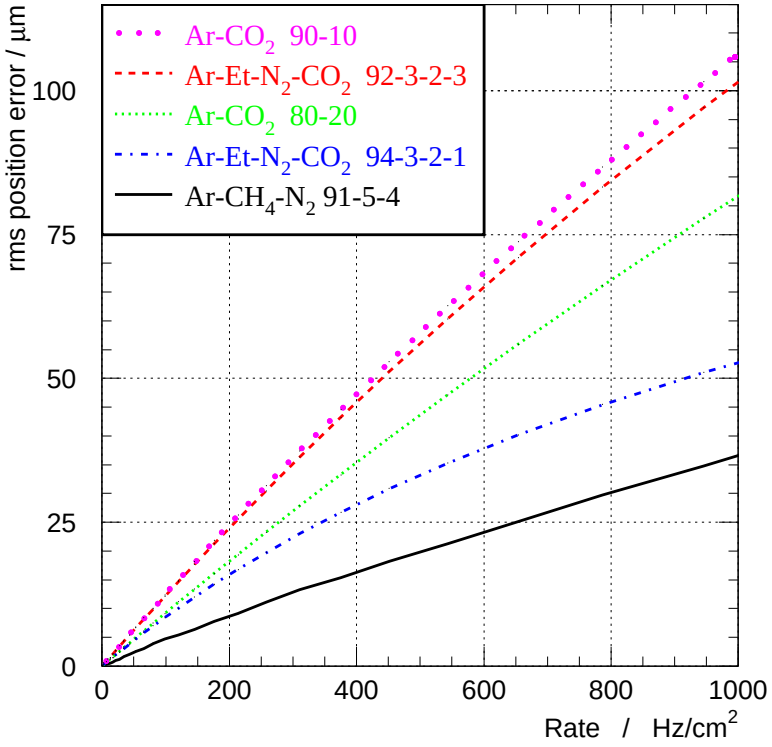

Figure 17: RMS of the spatial errors that result from taking the r-t relation for zero rate instead of one that would fit the actual rate (muon data, for photons take twice the rate).

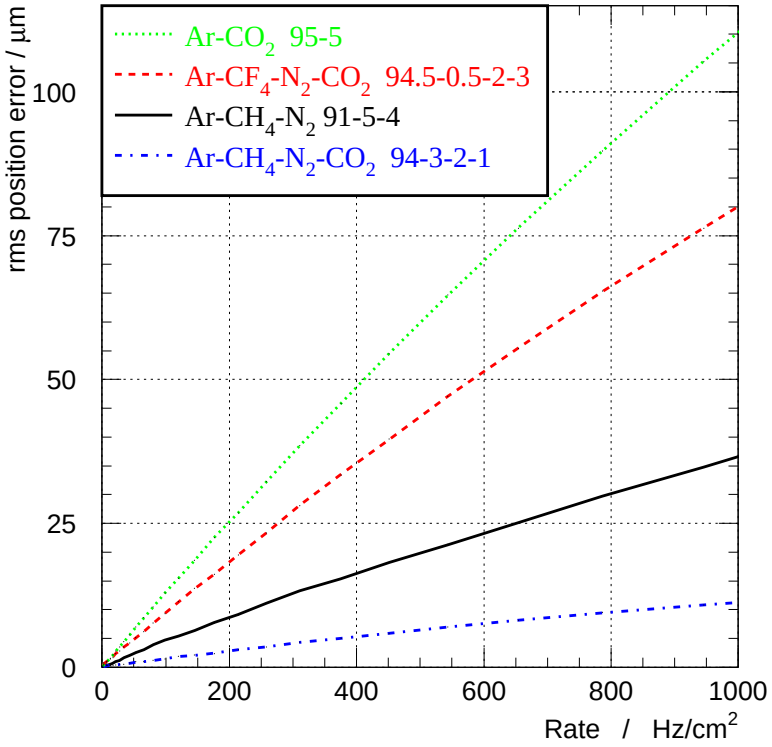

Figure 18: Calculation analogous to the one shown in the previous figure for new gases currently discussed for use in the MDTs. For comparison, the curve for DATCHA gas from fig.17 is added.

between the correct r-t relation (the one that would fit the actual rate) and the r-t relation determined for zero rate, averaged along the diameter of the tube. These numbers can be easily calculated knowing the drift velocity curves $v_{rate}(r)$, the result is shown in fig.17.
For most of the gases, the position errors are not negligible at the standard ATLAS rate of $100\,\mathrm{Hz/cm^2}$. The numbers are roughly increasing linearly if one wants to introduce a safety factor.
The error of Ar-CO_2 80-20 % looks much better compared to the other gases as one would expect from fig. 16. This is due to the very slow drift velocity (fig. 13) and the high maximum drift time (three times longer than e.g. DATCHA).
Fig. 18 shows the same calculations for new candidates of gases for the MDTs. In contrast to the DATCHA gas, the new ones seem to have much better ageing properties [15], but are still under study. Ar-CO_2 95-5 behaves similar to Ar-CO_2 90-10.
The most promising candidate is Ar-CH_4-N_2-CO_2 94-3-2-1, which has an excellent high rate behaviour, even better than the DATCHA gas. This is the same gas as in fig. 17, the one tested in our measurements, but with Ethane replaced by Methane. This does not change the linearity of the r-t relation, but because of the different quencher, the HV has to be chosen $\approx$ 700 V higher for the same gas gain. As described above, this reduces the high rate effects significantly.

The errors shown in figs. 17 and 18 could partly be compensated if it was possible to find always the correct r-t relation for the actual rate, e.g. by autocalibration. For ATLAS this would imply that the background rate has to be stable for some time.
What can not be compensated are fluctuations in the time between two hits. The distribution of these time is exponential, as was shown in fig. 6. At rates around 80 $\mathrm{Hz/cm^2}$ the mean time is in the order of the maximum ion drift time (4 ms). Whenever the time to the last hit is bigger than the maximum ion drift time, all positive ions are gone and the tube behaves as if rate was zero. At the rate of 80 $\mathrm{Hz/cm^2}$ this is true for 50% of the events. However, at that rate the mean changes to the r-t relation are not negligible. At time differences smaller than the mean value, the tube will behave as if rate $>$ actual rate. A more quantitative study of these fluctuations will be treated in a separate note.

7 Conclusion

Measurements of the gain reduction and changes of drift times have been done. For the gases that have been tested experimentally, a good agreement was found between measurements and calculation.
The behaviour of new candidate gases can be calculated if the ion mobility is known and if gas gain measurements are available.
The gas gain reduction of all possible gases for the MDTs is in the order of 10-20% at ATLAS conditions and can not be avoided.
The electric field for drifting electrons is changed because of space charges. Depending on which kind of gas is used, this may have almost no effect on the resolution (for linear gases) even at very high rates, or already big effects at ATLAS rates (non-linear gases).

References

[1] R.W. Hendricks, The Review of Scientific Instruments **40**, 1216 (1969)

[2] W. Diethorn, *A Methane Proportional Counter System for Natural Radiocarbon Measurements*, U. S. AEC Rep. NYO-6628 (1956)

[3] V. Rehmann *Messung der Gasverstärkung und Untersuchung von Alterungseffekten in Driftröhren* Diploma Thesis, Freiburg 1996

[4] B. Struck Tangstedt/Hamburg *Technical Manual DL 515 Flash-ADC VME Module*

[5] Schematics and Layout: F/B-Muonchamber Pre Amp FBPANIK-04, NIKHEF 1996

[6] D. Schaile, O. Schaile and J. Schwarz, Nucl. Instr. and Meth. A242 (1986) 247

[7] S.M. Tkaczyk et al, Nucl. Instr. and Meth. A270 (1988) 373

[8] F. Sauli *Principles of Operation of Multiwire Proportional and Drift Chambers* CERN 77-09 (1977)

[9] E.W. McDaniel and E.A. Mason, *The Mobility and Diffusion of Ions in Gases* (Wiley, New York 1973)

[10] W. Blum and L. Rolandi *Particle Detection with Drift Chambers* (Springer Berlin 1993)

[11] A. Biscossa et al, ATLAS Internal Note MUON-NO 196 (1997)

[12] The ATLAS Collaboration *Muon Spectrometer Technical Design Report* CERN/LHCC/97-22 (1997)

[13] G. Schultz, G. Charpak and F. Sauli, Rev. Phys. Appl.(France) **12**, 67 (1977)

[14] M. Aleksa, private communication

[15] M. Kollefrath et al., ATLAS Internal Note MUON-NO 176 (1997)

[16] S.F. Biagi, Nucl. Instr. and Meth. A283 (1989) 716